

3D Magnetic Resonance Electrical Impedance Tomography at 4T using Sensivity Matrix based Reconstruction

O. Birgul¹, L. T. Muftuler¹, M. J. Hamamura¹, and O. Nalcioglu¹

¹Tu and Yuen Center for Functional Onco Imaging, University of California, Irvine, CA, United States

Purpose

The difference between the conductivity of malignant tumors and the surrounding normal tissue provides a possible way to detect and specify different tumor types. The conductivity distribution can be found using magnetic resonance-electrical impedance tomography (MREIT) with a resolution higher than other conductivity imaging techniques [1]. In MREIT a current distribution is created within the object, resulting magnetic flux density is measured using MRI, and an inverse problem is solved to find the conductivity distribution using magnetic flux density measurements. MREIT reconstruction algorithms can be grouped into three: (1) current density based algorithms (that calculates current density from magnetic field during reconstruction), (2) gradient Bz algorithms (that uses first or second order derivative of magnetic flux density) and (3) sensitivity matrix based algorithms (that uses magnetic field directly). First group of algorithms requires rotation of the object inside the magnet, which is unpractical. Second group of algorithms are very sensitive to noise in the phase due to the derivative operator used. Sensitivity matrix approach is shown to perform better in noise; however, it requires storage and processing of large matrices. Several results have been presented for phantom and animal experiments using 2D sensitivity approach [1,2]. In 2D approximation, it is assumed that injected current is confined to the slice of interest and magnetic flux density measured from the same slice is used for reconstruction. In most experiments, however, injected currents will be distributed in all directions. Depending on the conductivity values of the adjacent slices, off-slice currents will contribute to the magnetic flux measurement and must be included in modeling. In this study, we conducted experiments with 3D phantoms and implemented a 3D sensitivity matrix reconstruction algorithm.

Methods

When low amplitude sinusoidal current is injected into an object, the resulting magnetic field accumulates additional phase in the MR images. A modified fast spin-echo sequence [3], where a 90° RF pulse is followed by a number of 180° (π) RF pulses, is used to measure the magnetic field. Phase induced in positive and negative current cycles would cancel out each other unless multiple π are used. By synchronizing successive π pulses to half cycles of the current, this phase shift accumulates and is given in the final image as $\phi(\mathbf{r}) = 4\gamma N \cdot \mathbf{b}(\mathbf{r}) / \omega$, where γ is the gyromagnetic ratio, N the number of cycles of injected current, $\mathbf{b}(\mathbf{r})$ the amplitude of z-component current-generated magnetic field at point \mathbf{r} , and ω the angular frequency of the injected current.

Once the magnetic field is measured, the inverse problem of calculating the internal conductivity distribution from these measurements is solved. Sensitivity based reconstruction algorithm is implemented in 3D. Uniform conductivity distribution is assumed and sensitivity matrix (\mathbf{S}) is calculated using a 3D finite element method (FEM). Sensitivity matrix gives the relation between $\Delta \mathbf{b}$ (the difference between measured magnetic flux density and the magnetic flux density corresponding to initial distribution) and $\Delta \sigma$ (the change with respect to initial) as $\Delta \mathbf{b} = \mathbf{S} \Delta \sigma$. Including Tikhonov regularization parameter, λ , the matrix equation becomes $(\mathbf{S}^T \mathbf{S} + \lambda \mathbf{I}) \Delta \sigma = \mathbf{S}^T \Delta \mathbf{b}$ where \mathbf{I} is the identity matrix. The matrix equation is solved for different values of λ using conjugate gradient method and the optimum regularization value is selected as the one minimizing the difference between measured and calculated magnetic flux densities.

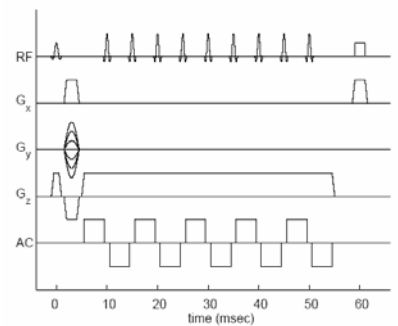


Fig 1. Pulse Sequence

Results

A 3D phantom was prepared using agarose powder (1gr/100mL) as background and a spherical shell filled with the same agarose gel. Due to insulator shell, the whole sphere acted as a nonconducting object. Four electrodes of size 0.5cm x 0.5cm were placed at the center of the cylinder every 90° as shown in Fig 2. Opposite pairs were used, giving two current injection profiles. A FEM mesh with 2399 nodes and 11781 tetrahedral elements was constructed. The magnetic flux density is calculated at a rectangular grid of 24x24x5, where 2300 of grid points falling into the cylindrical region. A total of 4600 measurements were used in image reconstruction. MR structural images for the 5 slices used are given in Fig. 3 (top row). Corresponding reconstructed conductivity images are presented in bottom row, dark region corresponding to insulating object.

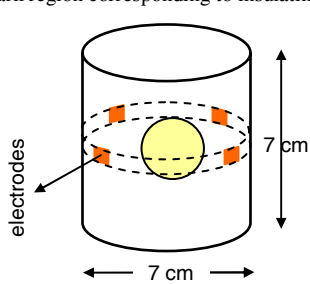


Fig 2. Phantom Definition

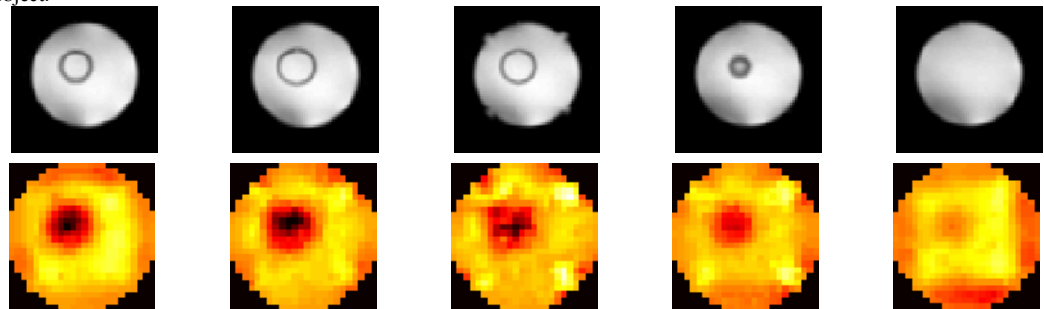


Fig 3. MR anatomical images (top row) and corresponding reconstructed conductivity images (bottom row)

Discussion

In this study, we demonstrated the feasibility of using 3D sensitivity matrix reconstruction in multi-slice magnetic resonance electrical impedance imaging. Although sensitivity matrix based reconstruction methods are computationally expensive, they perform well in the presence of noise. Previously, we used sensitivity matrix based reconstruction using 2D FEM. That approach ignores the contributions of currents in off-center slices leading to various artifacts in the conductivity images; conductivity values in the reconstructed slice could be under or overestimated, spatial resolution and point spread function could be compromised. In some cases the 'ghosts' of objects in other slices may even appear in the reconstructed slice depending on how the conductivity and resulting 3D current density is distributed in the object.

References

[1] Birgul O, et al. PMB, **51**, 5035-5049 (2006), [2] Muftuler L T, et al., TCRT **5** (4) 381-387 (2006). [3] Malich A, et al., Eur. Radiol, **10**, 1555-1561 (2000)

Acknowledgments

This research is supported in part by Department of Defense Award W81XWH-04-1-0446 and NIH/NCI Award R01 CA114210.